Experimental Study of Carbon Dioxide Absorption by Fe_2O_3@glutamine/NMP Nanofluid

Abbas Elhambakhsh
Shiraz University
Samira Heidari
Shiraz University
Peyman Keshavarz (pkeshavarz@shirazu.ac.ir)
Shiraz University https://orcid.org/0000-0001-5865-1269

Research Article

Keywords: CO2 absorption, Synthesis, Fe2O3, CO2 capture, NMP.

Posted Date: May 25th, 2021

DOI: https://doi.org/10.21203/rs.3.rs-498743/v1

Version of Record: A version of this preprint was published at Environmental Science and Pollution Research on August 3rd, 2021. See the published version at https://doi.org/10.1007/s11356-021-15650-3.

Abstract

In this study, the magnetic based nanoparticle (NP) of Fe_2O_3@glutamine ($C_5H_{10}N_2O_3$) was synthesized to improve the Fe_2O_3 properties in absorbing carbon dioxide (CO_2) using the base fluid of hydrous N-Methyl-2-pyrrolidone (NMP) solution (50wt.%), as a physically powerful CO_2 absorbent. To do this, several nano-NMP solutions, in different weight percentages of NPs were first prepared. Then, in a batch setup, the nano-NMP solutions were directly exposed to CO_2 gaseous (at the pressures of 20, 30, and 40 bar) to clarify the effects of the mass percentage of NPs and initial pressure on CO_2 absorption. Results clearly illustrated that Fe_2O_3 nanofluid was not stable more than 0.025 wt.%. However, Fe_2O_3@glutamine nanofluid was stable approximately two times more than Fe_2O_3 nanofluid due to the presence of glutamine as a hydrophilic agent in the structure of Fe_2O_3@glutamine. Moreover, in comparison to the base fluid (NMP solution), although Fe_2O_3 increased CO_2 absorption up to 9.14%, Fe_2O_3@glutamine NPs caused the CO_2 absorption to increase up to 19.41%, which can be determined as the chemical reactions of two amino groups in the glutamine structure with CO_2 and also higher Stability of Fe_2O_3@glutamine NPs compared to bare Fe_2O_3 NPs.

Introduction

Carbon dioxide (CO_2) is known as one of the most dangerous greenhouse gaseous which might bring several severe problems like climate change and acid rains if the amount of this exceeds 400 ppm in the atmosphere (Jiang et al. 2014; Lee et al. 2016; Rangwala 1996). Therefore, it is of importance to seek advanced techniques to decrease the quantity of this dangerous gas in the atmosphere.

There are several familiar approaches to reduce CO_2 content in the atmosphere, such as adsorption, absorption, cryonic, and using a membrane (Hafeez et al. 2020; Lee and Kang 2013; Lu et al. 2019; Wang et al. 2021; You et al. 2021). Benefiting from absorbents (like N-Methyl-2-pyrrolidone (NMP), diethanolamine (DEA), methyl diethanolamine (MDEA), and monoethanolamine (MEA)), which can physically or chemically capture CO_2 gaseous, is the most common approach used in the industries (Bohloul et al. 2014; Mumford et al. 2015; Rama et al. 2019; Seddigh et al. 2014; Zhang et al. 2018b). Since some absorbents have chemical reactions with CO_2, a chemical process is consequently required in the desorption step, causing a large sum of absorbents to be wasted. Further, chemical solvents seriously damage facilities due to the corrosion phenomenon, raising the operational costs (Ji et al. 2018; Wang et al. 2018). Therefore, although weaker bonds occur in physical absorption, using absorbents which can form physical absorption with CO_2 gaseous seems to be more economical (Rahmatmand et al. 2016). Benefiting from NPs as additives can significantly improve the strength of physical bonds and the yield of the absorption process. In an early NPs application in transportation, Choi and Eastman (Choi and Eastman 1995) improved thermal conductivity by 40% as a result of using NPs. In 2002, the impacts of liquid layering, Brownian motion, and NPs classification on thermal conductivity were investigated by Keblinski et al. (Keblinski et al. 2002) Prasher et al. (Prasher et al. 2006) showed the significant role of

NPs Brownian movements on thermal conductivity. After determining the resemblance and relation between the mass and heat transfer phenomenon, researchers investigated the NPs effects of mass transfer phenomenon. Krishnamurthy et al.(Krishnamurthy et al. 2006) revealed the fluorescein diffusion into the solution composed of Al_2O_3 NPs and water. They concluded that the nano-Al_2O_3 solution has more mass transfer nature (a maximum of 13 times) than the base fluid (water). Kim et al. (Kim et al. 2008) investigated the effect of NPs type on the capture of CO_2, which raised the CO_2 capture (to the maximum of 24%) of the base fluid (water) at atmospheric pressure in a bubble column system. Peyravi et al.(Peyravi et al. 2015) examined the CO_2 absorption in different nanofluids prepared from the water with each of silicon dioxide (SiO_2), iron(III) oxide (Fe_3O_4), carbon nanotube (CNT), and aluminum oxide (Al_2O_3) NPs. They concluded that all the mentioned nanofluids have more absorption rate than the base fluid (water) up to 25.9, 43.8, 38, and 3%, respectively. Lately, several types of researches have been accomplished to apply additives, like those with amino groups in their structures, on the NPs surfaces to chemically develop the absorption of CO_2 (Arshadi et al. 2019; Elhambakhsh et al. 2020b). Irani et al. (Irani et al. 2018) increased absorption (a maximum of 16%) in comparison to methyl diethanolamine (MDEA) solution utilizing polyethyleneimine functionalized HKUST-1 as an absorbent agent. Arshadi et al. (Arshadi et al. 2019) studied the impact of symmetric amine base magnetic-adsorbent nanodendritic on the CO_2 absorption in a bubble column at atmospheric pressure. Results revealed that modified NPs increased the absorption of CO_2 to the maximum of 70% in respect to water-based solvent. Although using NPs has turned into an fascinating solution in a wide domain of research projects accomplished to improve the absorption of CO_2, but in industrial scales, NPs dispersion is the most crucial problem (Zhang et al. 2018b), requiring a significant sum of power and ultrasonic irradiation (Schmerr and Song 2007). Further, the agglomeration and deposition tendency of NPs within a few hours (Zhang et al. 2018b). Accordingly, improving the stability of NPs is a key factor to increase the performance of CO_2 absorption in industrial applications.

Recently, a variety of NPs has been used to improve CO_2 absorption in solvents forming weak physical absorption with CO_2 at atmospheric conditions. Because there is minimal absorption capacity for the physical absorbents at down pressures (BURR and LYDDON 2009; Herzog 2003; Zhang et al. 2018a), the pressure is an underlying factor in industrial CO_2 capture projects. Therefore, working under high pressures can illustrate the real capacities of NPs in the absorption of CO_2, especially in industrial projects.

In the latest studies, researchers have shown the extraordinary effects of magnetic NPs on improving the absorption efficiency of CO_2 (Arshadi et al. 2019; Peyravi et al. 2015). Fe_2O_3 NPs with magnetic features can be collected by a magnetic field and reused easily. Large available surface to volume ratio, decent paramagnetic features, practical efficiency, low toxicity, and reusability are the vital properties of magnetic Fe_2O_3 NPs, causing most researchers to extensively use these NPs for CO_2 separation projects (Blaney 2007; Peyravi et al. 2015; Schätz et al. 2009). Existing two amino groups in glutamine structure can form carbamate during CO_2 absorption. Further, the primary aliphatic e-amino group in the glutamine

structure might cause positive charge explosion and increase the loading rate of CO_2. This positive charge might form a hydrogen bond with water, which favors deprotonation of CO_2-amino acid complex and facilitation of carbamate Therefore, in comparison to some other amino acids, glutamine has a higher capacity of CO_2 absorption, which can be attributed to the presence of nitrogen groups acting as a base groups to accept proton and form carbamate, respectively (Shen et al. 2015). The general reaction mechanism of CO_2 by amino acids is demonstrated in equation 1 (Zarei et al. 2020).

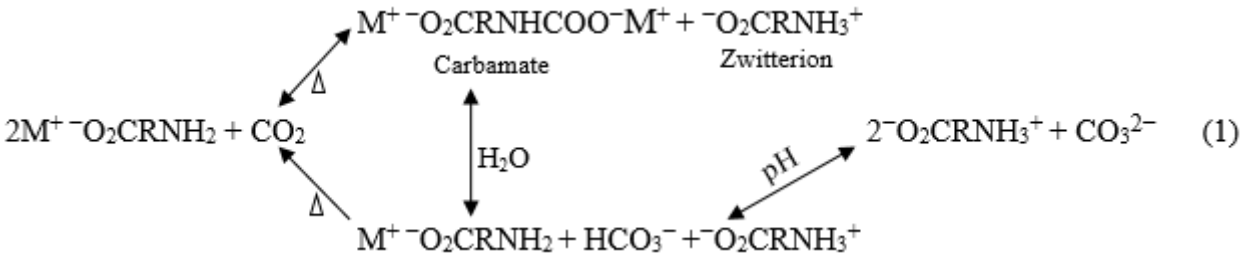

(1)

Herein, the NMP solution was employed as one of the most powerful absorbents physically absorbs CO_2, especially at high pressures. This solution can be used with other absorbents chemically and physically absorb CO_2 like water and Methyl diethanolamine (MDEA) (Elhambakhsh and Keshavarz 2020b). Benefiting Fe_2O_3@glutamine in NMP solution was performed based on two key points. Firstly, NMP is a safe and powerful absorbent of CO_2 without the significant problems of chemical absorbents of CO_2 (such as corrosion or recovery costs). Secondly, the performances of produced nanoparticles must be evaluated on an industrial absorbent of CO_2 under similar conditions (high-pressures) (Elhambakhsh and Keshavarz 2020a).

As a result, in this study, Iron(III) oxide (Fe_2O_3) and Iron(III) oxide@glutamine (Fe_2O_3@glutamine) NPs were synthesized by the co-precipitation approach and used as absorbents. Hydraulic NMP solution (50 wt.%) was used as the base fluid. The effect of Fe_2O_3 NPs and Fe_2O_3 functionalized with glutamine was investigated on the absorption of CO_2 in NMP solution. In addition, the stability of NPs in the base fluid was examined using Zeta potential (ZP) analysis. To the best of our knowledge, this is the first experience of applying glutamine as a CO_2 reactant on the structure of a nanoparticle to increase the CO_2 absorption capacity of NMP solution.

Experimental Section

2.1. Material and instruments

The aqueous base fluid was prepared from NMP (Sigma-Aldrich, 99.5%) and water (50 wt.%). Co-precipitation approach was used to synthesize Fe_2O_3 NPs from a solution prepared from $FeCl_3.6H_2O$ (Sigma-Aldrich, ≥99%) and $FeCl_2.4H_2O$ (Sigma-Aldrich, ≥99%). To improve the stability of NPs and the equilibrium absorption of NMP solution, L-glutamine (Sigma-Aldrich, ≥99%) was located on the surfaces of Fe_2O_3 NPs. NH_4OH (Sigma-Aldrich, 99.99%) and NaOH (Sigma-Aldrich, ≥98%) were used to adjust the

solution's pH. Ethanol (Sigma-Aldrich, ≥99.8%) was used as a reaction media and also for washing the precipitants. The pressure gauge indicators (Ashcroft 20893.0, ± 0.05%, USA) recorded the pressures of the containers. The required pure CO_2 (99%) was provided from Abughadre company, Fars, Iran. A vacuum pump (VE115N, China) was used to evacuate containers and lines from the air. To perform fourier transform infrared spectroscopy (FTIR) analysis, the Bruker spectrophotometer (model Tensor II, the accuracy of 5%, Germany) was used. Nanoparticle size and morphology of NPs were examined using transmission electron microscopy (TEM, Philips EM 208S, Germany) and scanning electron microscopy (SEM, TESCAN-Vega 3, Czech *Republic*). ZP analysis was accomplished using a Horiba device (Horiba, SZ- 100 DLS, Japan). An ultrasonic device (Tomy, UD-201, Japan) was employed to disperse NPs in NMP solution. C-Tab was used as a surfactant in ZP analysis. The specifications of employed chemicals are listed in Table 1.

Table 1

Utilized chemicals and their specifications.

Component	Linear Formula	CAS Registry Number	Molecular Weight ($g.mol^{-1}$)	Supplier	Purity
N-Methyl-2-pyrrolidone	C_5H_9NO	872-50-4	99.133	Sigma-Aldrich	99.5%
Ferric chloride hexahydrate	$FeCl_3.6H_2O$	10025-77-1	270.30	Sigma-Aldrich	≥99%
Ferrous chloride tetrahydrate	$FeCl_2.4H_2O$	13478-10-9	198.81	Sigma-Aldrich	≥99%
L-glutamine	$C_5H_{10}N_2O_3$	56-85-9	146.14	Sigma-Aldrich	≥99%
Ammonium hydroxide	NH_4OH	1336-21-6	35.046	Sigma-Aldrich	99.99%
Sodium hydroxide	NaOH	1310-73-2	40.00	Sigma-Aldrich	≥98%
Ethanol	CH_3CH_2OH	64-17-5	46.07	Sigma-Aldrich	≥99.8%
Carbon dioxide	CO_2	124-38-9	44.01	Abughadre company	99%

2.1.1. Preparation of Fe_2O_3 NPs

To synthesize $FeCl_3.6H_2O$ (0.1 M), Fe_2O_3 NPs and $FeCl_2.4H_2O$ (0.2 M) were simultaneously dispersed in 100 mL distilled water using an outside mechanical stirrer. The prepared solution was heated to a

maximum point of 80 °C. To moderate the pH of the solution to 8.5, NH_4OH was added to the prepared solution. The prepared Fe_2O_3 NPs were next collected from the solution using a powerful magnetic field. Distillated water and ethanol were utilized to wash the gathered NPs (for three times) and then the collected NPs were dried at 80 °C for 12 hours (Jeong et al. 2004).

2.1.2. Preparation of Fe_2O_3@glutamine NPs

To prepare Fe_2O_3@glutamine NPs, the synthesized Fe_2O_3 NPs and glutamine with a molar ratio of 1:20 were dissolved in a solution prepared from 100 mL of ethanol and 10 mL of deionized water. The prepared solution was stirred at 80 °C for 24 h. In the end, a strong magnetic field was used to gather Fe_2O_3@ glutamine NPs. The collected NPs were washed by distillated water and ethanol (for three times), and dried at 80 °C for 12 hours (Elhambakhsh et al. 2020a; Esmaeilpour et al. 2018; Ma et al. 2014).

2.2. Experimental methods

Fig. 1 reveals the high-pressure experimental setup for the absorption of CO_2. In each experiment, first, 20 mL of nanofluids-NMP solution was poured into container 2. Then, the containers and lines were vacuumed by the vacuum pump. Container 1 was next loaded by CO_2 gaseous to the desired pressure. To provide the desired temperature (308 K), the setup was kept in an oven for 2 hours before starting the experiments. The pressure of containers was consciously recorded by the pressure gauge indicators. Soave-Redlich-Kwong equation of state (Soave 1972) was utilized to account the initial moles of CO_2 based on the compressibility factor of CO_2 and pressure and volume of container 1. In the next step, all valves connecting containers 1 and 2 were opened and the secondary moles of CO_2 was computed based on the new volume, pressure, and compressibility factor of CO_2. In the end, the CO_2 absorption was calculated from equations 2 and 3.

$$n=PV/ZRT \quad (2)$$

Where n, P, V, Z, T, and R are the mole of CO_2, pressure, volume, compressibility factor, the temperature and universal gas constant, respectively.

$$\alpha = (n_i-n_t)/(V_{Liq} \times \rho_{Liq}) \quad (3)$$

where α is the absorbed CO_2 (mole) in 1 kg of absorbent ($mol.kg^{-1}$), n_i is the initial mole of CO_2, n_t is the mole of CO_2 at each specific time, is the nanofluids/NMP solution`s volume, and is the density of liquid phase.

2.3. Error analysis

To evaluate the error in the calculation of CO_2 absorption, uncertainty factor (u) was calculated from equation 4 (Holman 1966).

$$U(\alpha_t) = \left(\alpha_t \frac{u(P_o)}{RTZ_o}\right)^2 + \left(\alpha_t \frac{u(P_t)}{RTZ_t}\right)^2 + \left(\alpha_t \frac{u(V_{gas})}{V_{gas}}\right)^2 + \left(\alpha_t \frac{u(V_{Liq})}{V_{Liq}}\right)^2 + \left(\alpha_t \frac{u(T)}{T}\right)^2 \quad (4)$$

where u (P), u (V), and u (T) are constants of 0.00007 bar, 0.0000005 m^3, and 0.5 K, respectively, and is the amount of CO_2 absorbed at specific time of t ($mol.kg^{-1}$) (Holman 1966).

To obtained results, the highest value of is approximately 0.000008, which is very low as compared with the values of .

Results And Discussion

3.1. NPs characterization

3.1.1. FTIR analysis

FTIR analysis was performed to examine the molecular bonds of the synthesized Fe_2O_3 and Fe_2O_3@glutamine NPs (Bahmani et al. 2020; Rahmatmand et al. 2016). Based on Fig. 2, the vibration of Fe-O was revealed between 540-560 cm-1, and the peaks between 3100-3400 cm-1 were related to N-H bonds due to the presence of amino groups in the structure of Fe_2O_3@glutamine (Branca et al. 2016; Esmaeilpour et al. 2018; Hampton et al. 2010; Patel et al. 2009; Rahmatmand et al. 2016; Singh 2008; Zandahvifard et al. 2021).

3.1.2. TEM and SEM analyses

The size and morphology of NPs were investigated using TEM and SEM analyses, respectively. According to Fig.3, all synthesized and functionalized NPs had a spherical structure. Most Fe_2O_3 NPs had the average diameters of 5-13 nm. Besides, Fe_2O_3@glutamine NPs were more significant in diameter in comparison to Fe_2O_3 NPs with an average diameter of 9-17 nm. The NPs characteristics were shown in Table 2.

Table 2

NPs Characterization.

Name	Color	Morphology	Average particle size, nm
Fe_2O_3	Dark brown	Spherical	5-13
Fe_2O_3@glutamine	Dark brown	Spherical	9-17

3.1.3. Stability of NPs

Generally, there is a high tendency for NPs to agglomerate and sediment in the based solvent. According to the literature, ZP analysis is a well-known approach to determine the stability of NPs (Liao et al. 2009; Shadanfar et al. 2021; Tso et al. 2010; Wang et al. 2016). Based on ZP results (Ali et al. 2018), NPs will have high, acceptable, medium, and weak stability if the absolute ZP is more than 60 mV, between 30-60 mV, between 20-30 mV, and between 0-20 mV, respectively. Table 3 presents the ZP of nanofluids in different concentrations. Regarding the pH of NMP solution (5.5) and Table 3, NPs did not have a real effect on the pH of the solution, proving that the ZP was not affected by pH.

Table 3

ZP analysis for Fe_2O_3 and Fe_2O_3@glutamine at different concentrations.

Nano fluid	pH	Absolute ZP after 8 hours (mV)(±2)	Status
Fe_2O_3 (0.01 wt.%)	5.5	40.1	Stable
Fe_2O_3 (0.025 wt.%)	5.5	29	Stable
Fe_2O_3 (0.05 wt.%)	5.5	21.9	Stable
Fe_2O_3 (0.075 wt.%)	5.6	17.6	Unstable
Fe_2O_3@glutamine (0.01 wt.%)	5.5	53	Stable
Fe_2O_3@glutamine (0.025 wt.%)	5.5	44.2	Stable
Fe_2O_3@glutamine (0.05 wt.%)	5.6	35.5	Stable
Fe_2O_3@glutamine (0.075 wt.%)	5.6	23.8	Unstable

As shown in Table 2, Fe_2O_3 NPs had hydrophobic characteristics and were stable up to approximately 0.025 wt.%. Beyond this weight percentage of NPs, the ZP was less than the stability of nanofluids (lower than 30 mV). Fe_2O_3@glutamine NPs were stable as twice as Fe_2O_3 NPs and could be dispersed in NMP solution to the maximum of 0.05 wt.% without plummeting into the unstable range of zeta potential.

3.2. CO_2 absorption

3.2.1. CO_2 absorption mechanisms

CO_2 absorption can be improved using NPs according to different absorption mechanisms. In one of these mechanisms, the CO_2 mass transfer in the base fluid will be facilitated as a result of Brownian motions of NPs, acting as micro-mixers in the solution (Brownian motion theory). The high surface area of NPs is another reason for the CO_2 absorption of nano solutions. Further, micro-movements of NPs can cause the CO_2 molecules to be taken on the NPs surfaces and transferred to the bulk solution (Shuttle

effect theory). According to the last literacy, irregular movements of NPs break large CO_2 bubbles into smaller ones, increasing the bubbles' surface area, and consequently the mass transfer of CO_2 (Bubble breaking theory) (Krishnamurthy et al. 2006; Nabipour et al. 2017; Zare et al. 2019). The schematic of the defined mechanisms is shown in Fig. 4.

In this study, it was tried to increase the CO_2 absorption capacity of the Fe_2O_3/NMP nano solution using glutamine amino acid. The absorption capacity of the fundamental solution was improved using NH_2 agents as chemical absorbents of CO_2. Therefore, the modified Fe_2O_3 NPs increased the CO_2 absorption in both chemical and physical mechanisms.

3.2.2. Fe_2O_3 nanofluids

Fig.5 illustrates the quantity of CO_2 absorption (α) in NMP solution and Fe_2O_3 nano solution including different weight percentages of NP (0.01, 0.025, 0.05, and 0.075 wt.%) at various initial pressures (20, 30, and 40 bar). Results revealed that pressure had an affirmative effect on the equilibrium absorption of CO_2 in such a way that the maximum amount was obtained at 40 bar. For all examined pressures, the optimum weight percentage of Fe_2O_3 NPs was found to be 0.025 wt.%. Furthermore, the maximum amount of CO_2 equilibrium absorption for NMP solution and Fe_2O_3 nano solution was 1.21 and 1.32 $mol.kg^{-1}$, respectively. Therefore, Fe_2O_3 nanofluids increased the CO_2 absorption of the base fluid to the maximum of 9.14% at the optimum concentration of NPs concentration. It proves that the NPs using only physical mechanisms like Brownian motion or grazing effect (Rahmatmand et al. 2016) can slightly improve the CO_2 absorption, which is not effective in industrial conditions.

Although it was expected to have more CO_2 absorption at a higher weight percentage of NPs, there was lower CO_2 absorption at NPs concentration more than 0.025 wt.%. This can be credited to the high NPs tendency to agglomerate and sediment at their high weight percentages (Peyravi et al. 2015; Rahmatmand et al. 2016). The instability of Fe_2O_3 nanofluids was discussed in the previous section (3.1.3).

3.2.3. Fe_2O_3@glutamine

Fig. 6 shows the equilibrium absorption of CO_2 in Fe_2O_3@glutamine nanosolutions at the pressures of 20, 30, and 40 bar. As can be seen, similar to Fe_2O_3, the highest CO_2 absorption was observed at 40 bar for Fe_2O_3@glutamine nano solution. Furthermore, the optimum weight percentage of NPs was found to be 0.05 wt.% in which the CO_2 absorption was increased to the maximum of 19.41% in comparison to the NMP solution.

3.2.4. Comparison of CO_2 absorption capacities for Fe_2O_3 and Fe_2O_3@glutamine nano solutions in

optimum concentrations

Considering Fig. 7, Fe_2O_3@glutamine nano solution had more ability in absorbing CO_2 than Fe_2O_3 nano solution which can be attributed to both physical mechanisms (Brownian motion, grazing effect, etc.) and chemical reactions among CO_2 molecules and amino groups existing in the glutamine structure. In addition, due to the hydrophilic properties of amino acids (Elhambakhsh et al. 2020a) Fe_2O_3@glutamine NPs could be employed at higher concentrations (0.05 wt.%) than bare Fe_2O_3 NPs. Therefore, Fe_2O_3@glutamine nano solutions have a higher potential to increase CO_2 absorption than Fe_2O_3 nano solutions.

The details of CO_2 absorption experiments in each time are mentioned in supplementary information section (Table S1-S9).

Conclusions

In this study, Fe_2O_3 and Fe_2O_3@glutamine NPs were first synthesized by co-precipitation approach and then were used to increase the absorption of CO_2 in NMP solution as the base fluid at high pressures of 20, 30, and 40 bar. Results revealed that, although Fe_2O_3 nano solution had little effect on CO_2 absorption which was due to the weak physical absorption, Fe_2O_3@glutamine nano solution caused CO_2 absorption to increase up to 19.41 and 9.4% more than NMP solution and NMP based Fe_2O_3 nano solution, respectively, which was due to the chemical reactions among amino groups of glutamine with CO_2 molecules.

Declarations

1. **Ethical Approval:** Not applicable.
2. **Consent to Participate:** Not applicable.
3. **Consent to Publish:** Not applicable.
4. **Authors Contributions:**

- **Abbas Elhambakhsh:** Methodology, Software, Data curation, Investigation, Resources, and Writing - review & editing.
- **Samira Heidari:** Validation, Formal analysis, and Writing - original draft.
- **Peyman Keshavarz:** Conceptualization, Visualization, Supervision, Project administration, and Funding acquisition.

5. **Funding:** This work was financially supported by Shiraz University, Shiraz, Iran (No. 7134851154).
6. **Competing Interests:** The authors declare that they have no competing interests.
7. **Availability of data and materials:** All data generated or analysed during this study are included in this published article (and its supplementary information files).

References

1. Ali N, Teixeira JA, Addali A (2018) A review on nanofluids: fabrication, stability, and thermophysical properties Journal of Nanomaterials 2018
2. Arshadi M, Taghvaei H, Abdolmaleki M, Lee M, Eskandarloo H, Abbaspourrad A (2019) Carbon dioxide absorption in water/nanofluid by a symmetric amine-based nanodendritic adsorbent Applied Energy 242:1562-1572 doi:https://doi.org/10.1016/j.apenergy.2019.03.105
3. Bahmani M, Mowla D, Esmaeilzadeh F, Ghaedi M (2020) BiFeO3–BiOI impregnation to UiO-66 (Zr/Ti) as a promising candidate visible-light-driven photocatalyst for boosting urea photodecomposition in a continuous flow-loop thin-film slurry flat-plate photoreactor Journal of Solid State Chemistry:121304
4. Blaney L (2007) Magnetite (Fe3O4): Properties, synthesis, and applications
5. Bohloul M, Vatani A, Peyghambarzadeh S (2014) Experimental and theoretical study of CO2 solubility in N-methyl-2-pyrrolidone (NMP) Fluid Phase Equilibria 365:106-111
6. Branca C, D'Angelo G, Crupi C, Khouzami K, Rifici S, Ruello G, Wanderlingh U (2016) Role of the OH and NH vibrational groups in polysaccharide-nanocomposite interactions: A FTIR-ATR study on chitosan and chitosan/clay films Polymer 99:614-622
7. BURR B, LYDDON L (2009) Which physical solvent is best for acid gas removal?: Four common solvents are compared: Gas processing developments Hydrocarbon processing (International ed) 88
8. Choi SU, Eastman JA (1995) Enhancing thermal conductivity of fluids with nanoparticles. Argonne National Lab., IL (United States),
9. Elhambakhsh A, Keshavarz P (2020a) Effects of Different Amin-based Core-Shell Magnetic NPs on CO2 Capture using NMP Solution at High Pressures Journal of Natural Gas Science and Engineering:103645
10. Elhambakhsh A, Keshavarz P (2020b) Effects of different amin-based core-shell magnetic NPs on CO2 capture using NMP solution at high pressures Journal of Natural Gas Science and Engineering 84:103645 doi:https://doi.org/10.1016/j.jngse.2020.103645
11. Elhambakhsh A, Keshavarz P (2020c) Investigation of Carbon Dioxide Absorption Using Different Functionalized Fe3O4 Magnetic Nanoparticles Energy & Fuels doi:https://doi.org/10.1021/acs.energyfuels.0c00234
12. Elhambakhsh A, Zaeri MR, Mehdipour M, Keshavarz P (2020a) Synthesis of Different Modified Magnetic Nanoparticles for Selective Physical/Chemical Absorption of CO2 in a Bubble Column Reactor Journal of Environmental Chemical Engineering:104195 doi:https://doi.org/10.1016/j.jece.2020.104195
13. Elhambakhsh A, Zaeri MR, Mehdipour M, Keshavarz P (2020b) Synthesis of different modified magnetic nanoparticles for selective physical/chemical absorption of CO2 in a bubble column reactor Journal of Environmental Chemical Engineering 8:104195 doi:https://doi.org/10.1016/j.jece.2020.104195

14. Esmaeilpour M, Zahmatkesh S, Fahimi N, Nosratabadi M (2018) Palladium nanoparticles immobilized on EDTA-modified Fe3O4@ SiO2 nanospheres as an efficient and magnetically separable catalyst for Suzuki and Sonogashira cross-coupling reactions Applied Organometallic Chemistry 32:e4302 doi:https://doi.org/10.1002/aoc.4302
15. Hafeez S et al. (2020) CO 2 capture using membrane contactors: a systematic literature review Frontiers of Chemical Science and Engineering:1-35
16. Hampton C, Demoin D, Glaser RE (2010) Vibrational spectroscopy tutorial: sulfur and phosphorus University of missouri, fall
17. Herzog H (2003) Assessing the Feasibility of Capturing CO2 from the Air Massachusetts Institute of Technology, Laboratory for Energy and the Environment, Publication No LFEE 2
18. Holman J (1966) Experimental Methods for Engineers, 37-40. New York: McGraw-Hill Book,
19. Irani V, Tavasoli A, Maleki A, Vahidi M (2018) Polyethyleneimine-functionalized HKUST-1/MDEA nanofluid to enhance the absorption of CO2 in gas sweetening process International Journal of Hydrogen Energy 43:5610-5619 doi:https://doi.org/10.1016/j.ijhydene.2018.01.120
20. Jeong JR, Lee SJ, Kim JD, Shin SC (2004) Magnetic properties of γ-Fe2O3 nanoparticles made by coprecipitation method physica status solidi (b) 241:1593-1596
21. Ji L et al. (2018) Integrated absorption-mineralisation for low-energy CO2 capture and sequestration Applied Energy 225:356-366
22. Jiang J, Zhao B, Zhuo Y, Wang S (2014) Experimental study of CO2 absorption in aqueous MEA and MDEA solutions enhanced by nanoparticles International Journal of greenhouse gas control 29:135-141
23. Keblinski P, Phillpot S, Choi S, Eastman J (2002) Mechanisms of heat flow in suspensions of nano-sized particles (nanofluids) International journal of heat and mass transfer 45:855-863 doi:https://doi.org/10.1016/S0017-9310(01)00175-2
24. Kim W-g, Kang HU, Jung K-m, Kim SH (2008) Synthesis of silica nanofluid and application to CO2 absorption Separation Science and Technology 43:3036-3055 doi:https://doi.org/10.1080/01496390802063804
25. Krishnamurthy S, Bhattacharya P, Phelan P, Prasher R (2006) Enhanced mass transport in nanofluids Nano letters 6:419-423 doi:https://doi.org/10.1021/nl0522532
26. Lee JW, Kang YT (2013) CO2 absorption enhancement by Al2O3 nanoparticles in NaCl aqueous solution Energy 53:206-211 doi:https://doi.org/10.1016/j.energy.2013.02.047
27. Lee JW, Pineda IT, Lee JH, Kang YT (2016) Combined CO2 absorption/regeneration performance enhancement by using nanoabsorbents Applied energy 178:164-176
28. Liao D, Wu G, Liao B (2009) Zeta potential of shape-controlled TiO2 nanoparticles with surfactants Colloids and Surfaces A: Physicochemical and Engineering Aspects 348:270-275
29. Lu J-G et al. (2019) CO 2 capture by ionic liquid membrane absorption for reduction of emissions of greenhouse gas Environmental Chemistry Letters 17:1031-1038

30. Ma Y-H, Peng H-Y, Yang R-X, Ni F (2014) Preparation of Lysine-Coated Magnetic Fe Asian Pacific Journal of Cancer Prevention 15:8981-8985
31. Mumford KA, Wu Y, Smith KH, Stevens GW (2015) Review of solvent based carbon-dioxide capture technologies Frontiers of Chemical Science and Engineering 9:125-141 doi:10.1007/s11705-015-1514-6
32. Nabipour M, Keshavarz P, Raeissi S (2017) Experimental investigation on CO2 absorption in Sulfinol-M based Fe3O4 and MWCNT nanofluids International Journal of Refrigeration 73:1-10 doi:https://doi.org/10.1016/j.ijrefrig.2016.09.010
33. Patel D, Chang Y, Lee GH (2009) Amino acid functionalized magnetite nanoparticles in saline solution Current Applied Physics 9:S32-S34 doi:https://doi.org/10.1016/j.cap.2008.08.027
34. Peyravi A, Keshavarz P, Mowla D (2015) Experimental investigation on the absorption enhancement of CO2 by various nanofluids in hollow fiber membrane contactors Energy & Fuels 29:8135-8142 doi:https://doi.org/10.1021/acs.energyfuels.5b01956
35. Prasher R, Bhattacharya P, Phelan PE (2006) Brownian-motion-based convective-conductive model for the effective thermal conductivity of nanofluids Journal of heat transfer 128:588-595 doi:https://doi.org/10.1115/1.2188509
36. Rahmatmand B, Keshavarz P, Ayatollahi S (2016) Study of absorption enhancement of CO2 by SiO2, Al2O3, CNT, and Fe3O4 nanoparticles in water and amine solutions Journal of Chemical & Engineering Data 61:1378-1387 doi:https://doi.org/10.1021/acs.jced.5b00442
37. Rama S, Zhang Y, Tchuenbou-Magaia F, Ding Y, Li Y (2019) Encapsulation of 2-amino-2-methyl-1-propanol with tetraethyl orthosilicate for CO2 capture Frontiers of Chemical Science and Engineering 13:672-683 doi:10.1007/s11705-019-1856-6
38. Rangwala HA (1996) Absorption of carbon dioxide into aqueous solutions using hollow fiber membrane contactors Journal of Membrane Science 112:229-240
39. Schätz A, Hager M, Reiser O (2009) Cu (II)-Azabis (oxazoline)-Complexes Immobilized on Superparamagnetic Magnetite@ Silica-Nanoparticles: A Highly Selective and Recyclable Catalyst for the Kinetic Resolution of 1, 2-Diols Advanced Functional Materials 19:2109-2115
40. Schmerr L, Song J-S (2007) Ultrasonic nondestructive evaluation systems. Springer,
41. Seddigh E, Azizi M, Sani ES, Mohebbi-Kalhori D (2014) Investigation of Poly (ether-b-amide)/Nanosilica Membranes for CO 2/CH 4 Separation Chinese Journal of Polymer Science 32:402-410
42. Shadanfar H, Elhambakhsh A, Keshavarz P (2021) Air dehumidification using various TEG based nano solvents in hollow fiber membrane contactors Heat and Mass Transfer doi:10.1007/s00231-021-03057-2
43. Shen S, Yang Y-n, Wang Y, Ren S, Han J, Chen A (2015) CO2 absorption into aqueous potassium salts of lysine and proline: density, viscosity and solubility of CO2 Fluid Phase Equilibria 399:40-49
44. Singh J (2008) FTIR and Raman spectra and fundamental frequencies of biomolecule: 5-methyluracil (thymine) Journal of Molecular Structure 876:127-133

doi:https://doi.org/10.1016/j.molstruc.2007.06.014

45. Soave G (1972) Equilibrium constants from a modified Redlich-Kwong equation of state Chemical engineering science 27:1197-1203 doi:https://doi.org/10.1016/0009-2509(72)80096-4
46. Tso C-p, Zhung C-m, Shih Y-h, Tseng Y-M, Wu S-c, Doong R-a (2010) Stability of metal oxide nanoparticles in aqueous solutions Water Science and Technology 61:127-133
47. Wang D, Li S, Liu F, Gao L, Sui J (2018) Post combustion CO2 capture in power plant using low temperature steam upgraded by double absorption heat transformer Applied Energy 227:603-612
48. Wang T, Yu W, Liu F, Fang M, Farooq M, Luo Z (2016) Enhanced CO2 absorption and desorption by monoethanolamine (MEA)-based nanoparticle suspensions Industrial & Engineering Chemistry Research 55:7830-7838 doi:https://doi.org/10.1021/acs.iecr.6b00358
49. Wang W, Wei Y, Fan J, Cai J, Lu Z, Ding L, Wang H (2021) Recent progress of two-dimensional nanosheet membranes and composite membranes for separation applications Frontiers of Chemical Science and Engineering doi:10.1007/s11705-020-2016-8
50. You L et al. (2021) Molecular level understanding of CO2 capture in ionic liquid/polyimide composite membrane Frontiers of Chemical Science and Engineering doi:10.1007/s11705-020-2009-7
51. Zandahvifard MJ, Elhambakhsh A, Ghasemi MN, Esmaeilzadeh F, Parsaei R, Keshavarz P, Wang X (2021) Effect of Modified Fe3O4 Magnetic NPs on the Absorption Capacity of CO2 in Water, Wettability Alteration of Carbonate Rock Surface, and Water–Oil Interfacial Tension for Oilfield Applications Industrial & Engineering Chemistry Research doi:https://doi.org/10.1021/acs.iecr.0c04857
52. Zare P, Keshavarz P, Mowla D (2019) Membrane Absorption Coupling Process for CO2 Capture: Application of water-based ZnO, TiO2, and MWCNT nanofluids Energy & Fuels doi:https://doi.org/10.1021/acs.energyfuels.8b03972
53. Zarei A, Hafizi A, Rahimpour M, Raeissi S (2020) Carbon dioxide absorption into aqueous potassium salt solutions of glutamine amino acid Journal of Molecular Liquids 301:111743 doi:https://doi.org/10.1016/j.molliq.2019.111743
54. Zhang H, Liu R, Ning T, Lal R (2018a) Higher CO 2 absorption using a new class of calcium hydroxide (Ca (OH) 2) nanoparticles Environmental Chemistry Letters 16:1095-1100 doi:https://doi.org/10.1007/s10311-018-0729-4
55. Zhang Z, Cai J, Chen F, Li H, Zhang W, Qi W (2018b) Progress in enhancement of CO2 absorption by nanofluids: A mini review of mechanisms and current status Renewable energy 118:527-535 doi:https://doi.org/10.1016/j.renene.2017.11.031

Figures

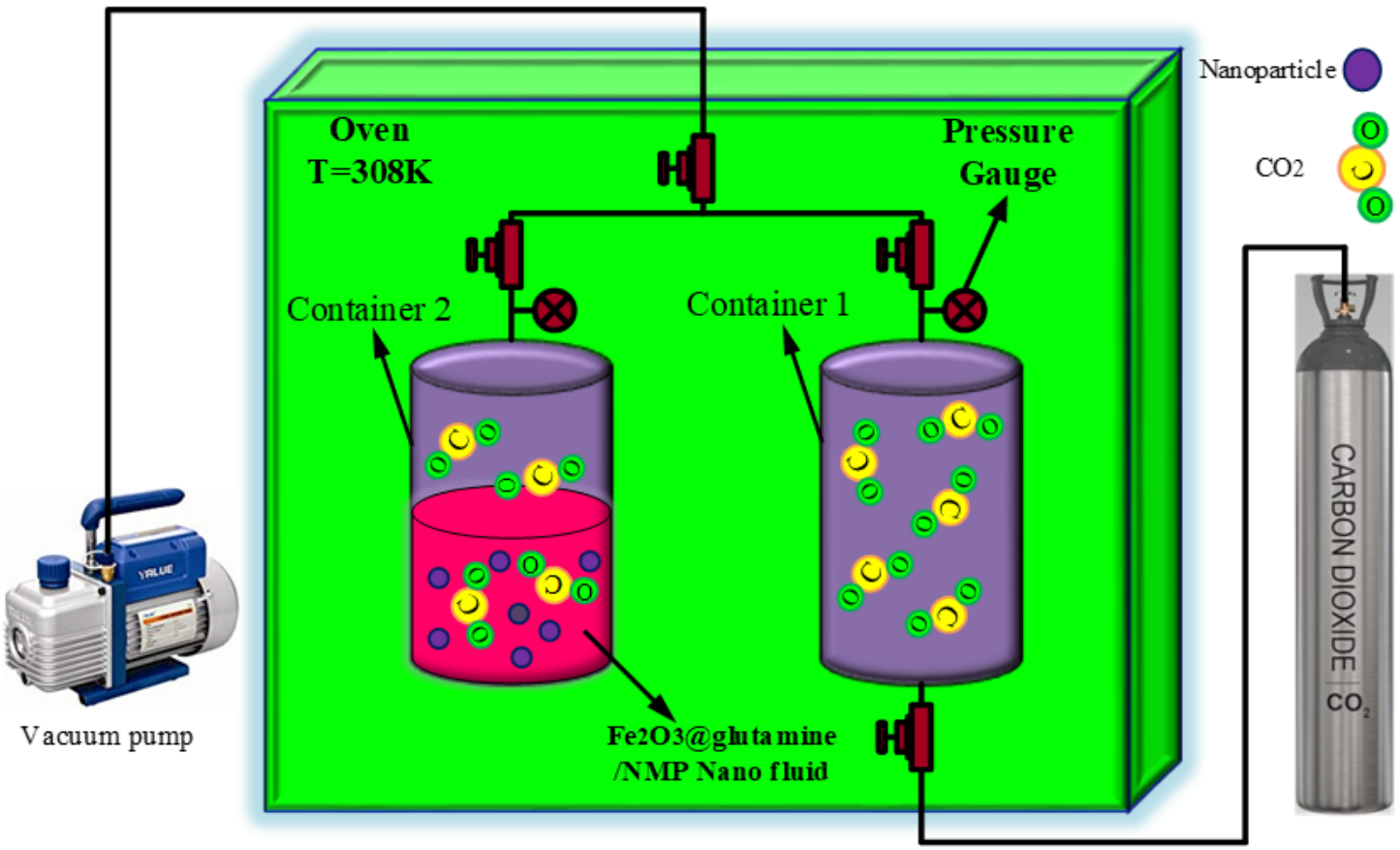

Figure 1

Schematic diagram of experimental mode (Elhambakhsh and Keshavarz 2020c).

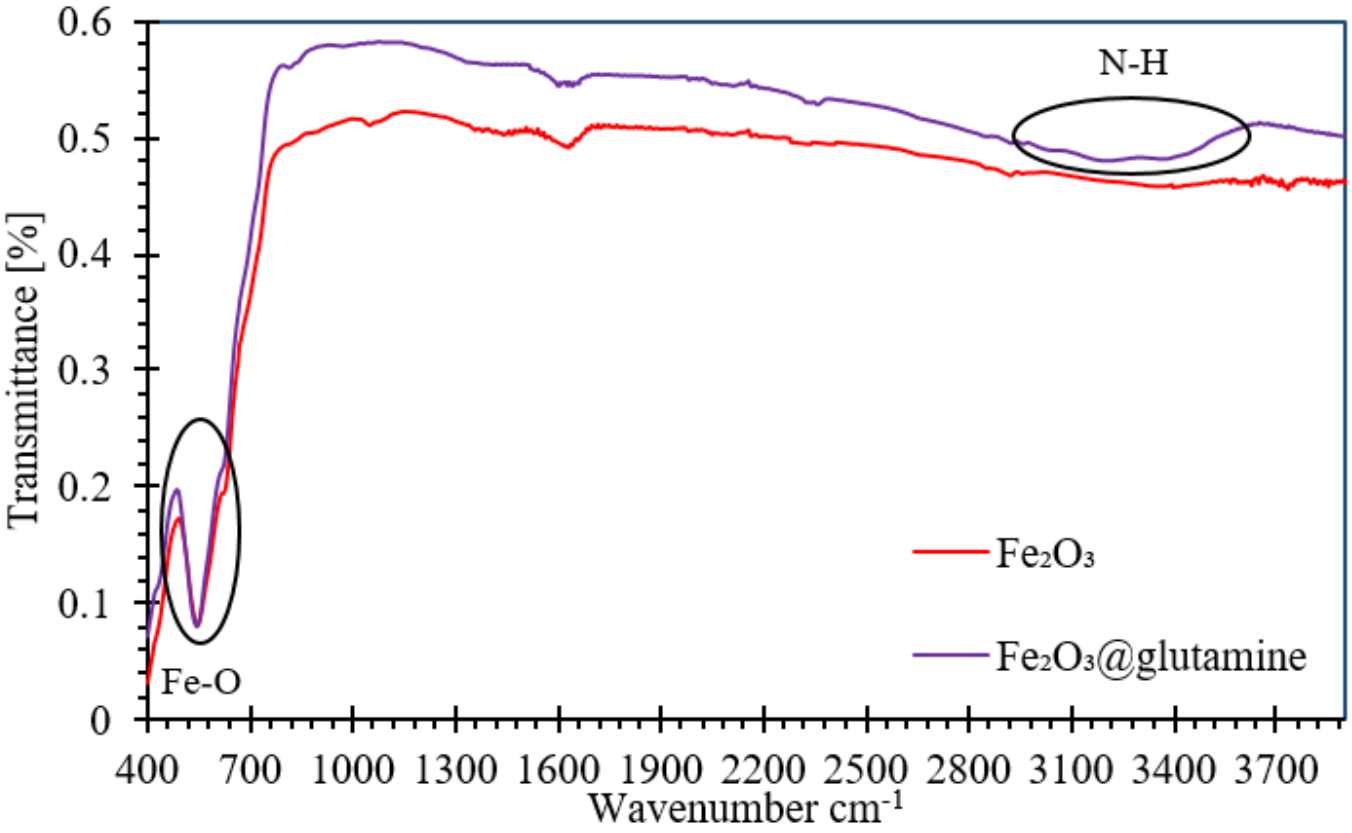

Figure 2

FTIR spectra of Fe2O3 and Fe2O3@glutamine NPs.

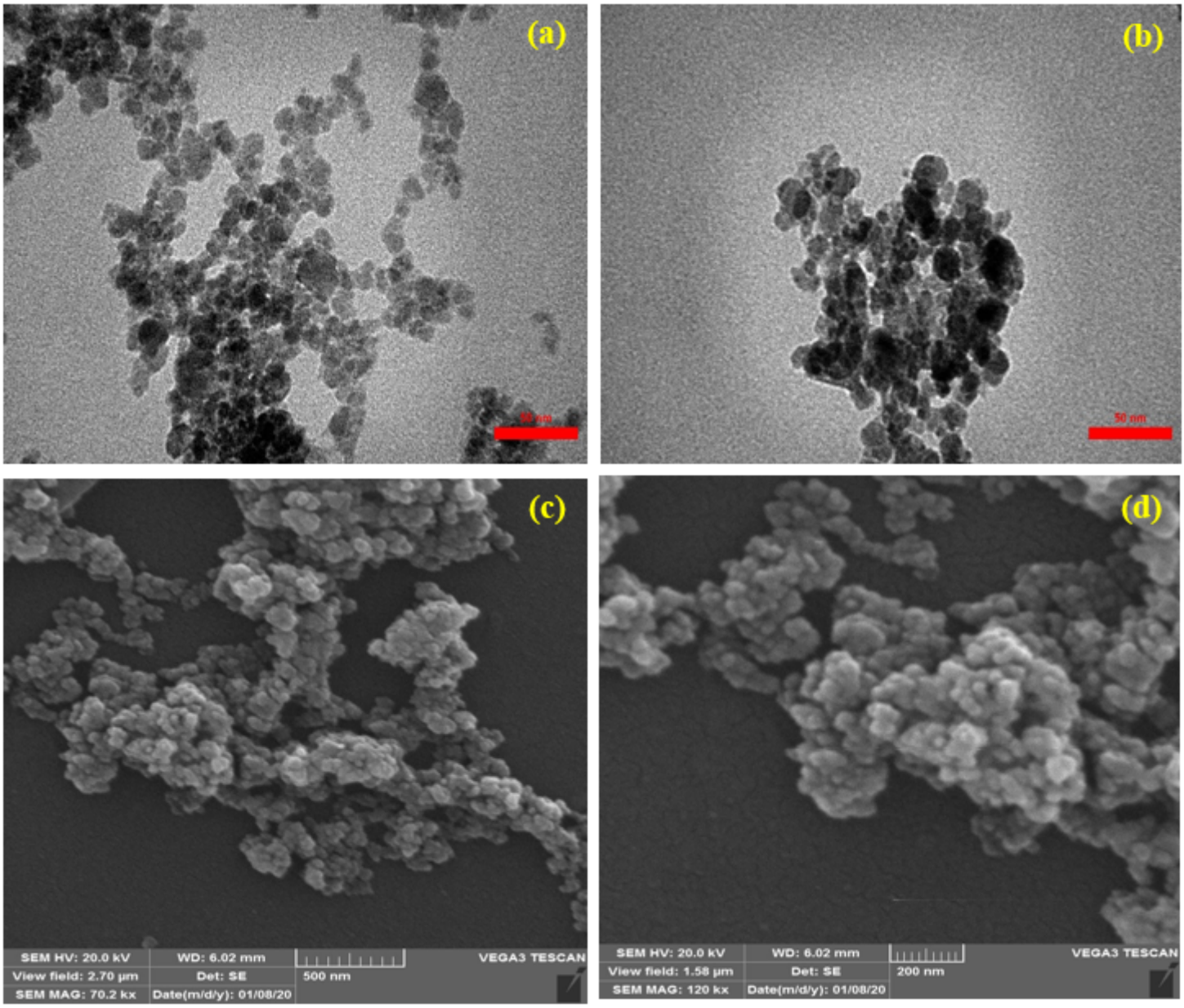

Figure 3

TEM images of a) Fe2O3, and b) Fe2O3@glutamine; SEM images of c) Fe2O3, and d) Fe2O3@glutamine, respectively.

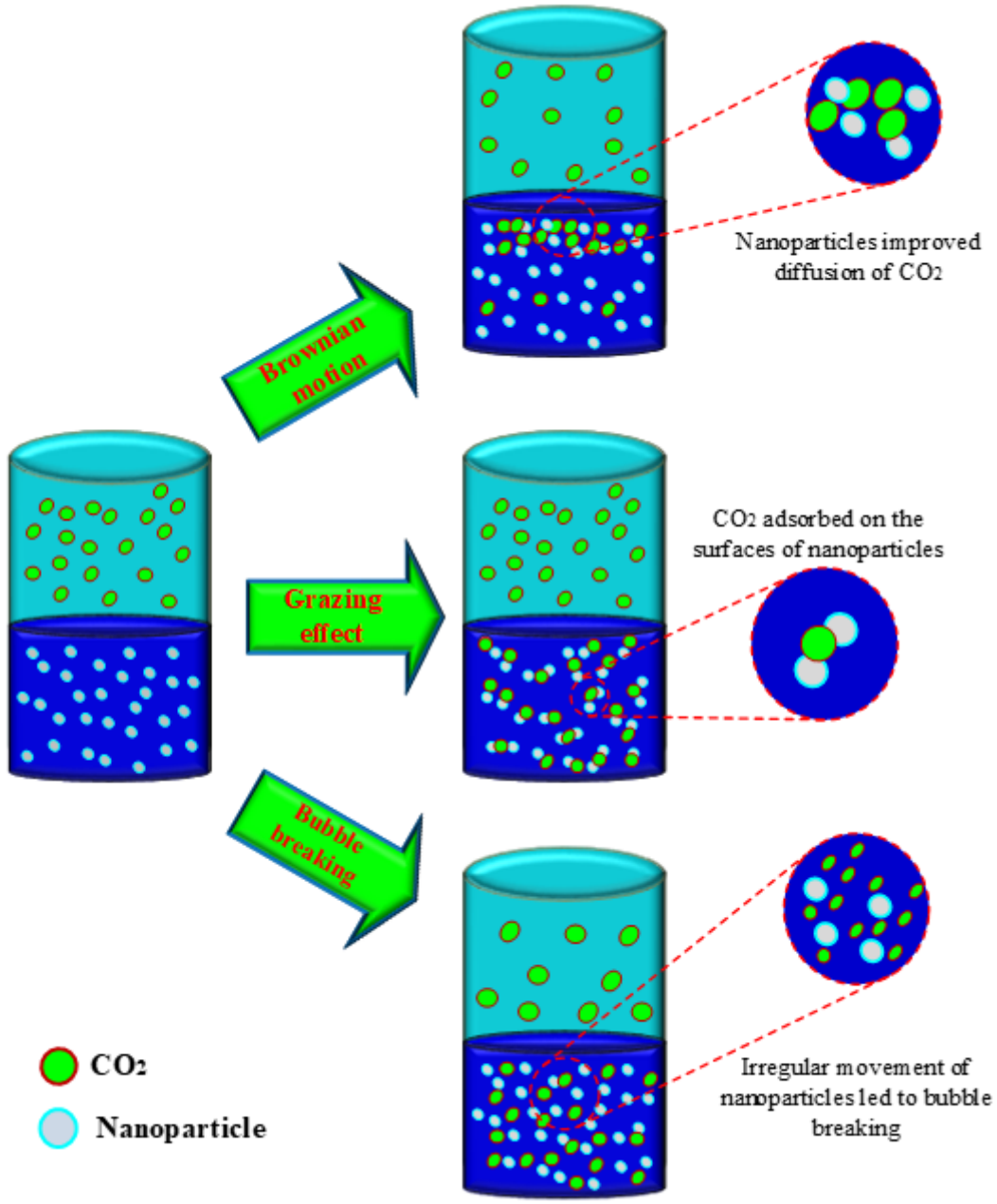

Figure 4

Schematic of effective mechanisms of NPs in CO2 absorption enhancement.

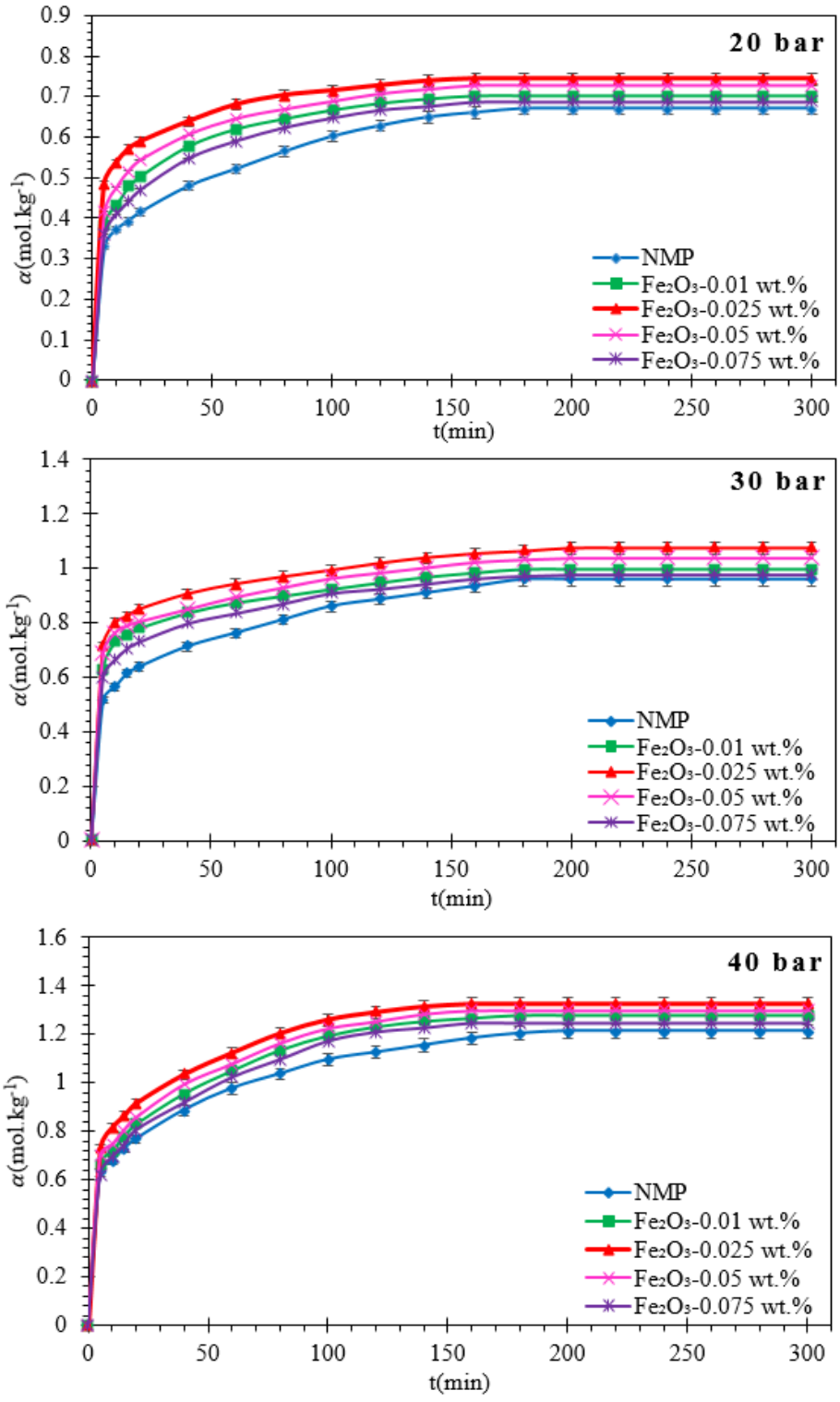

Figure 5

Influence of Fe2O3 NPs on CO2 absorption of NMP solution at the initial presssure of 20, 30, and 40 bar (T=308 K).

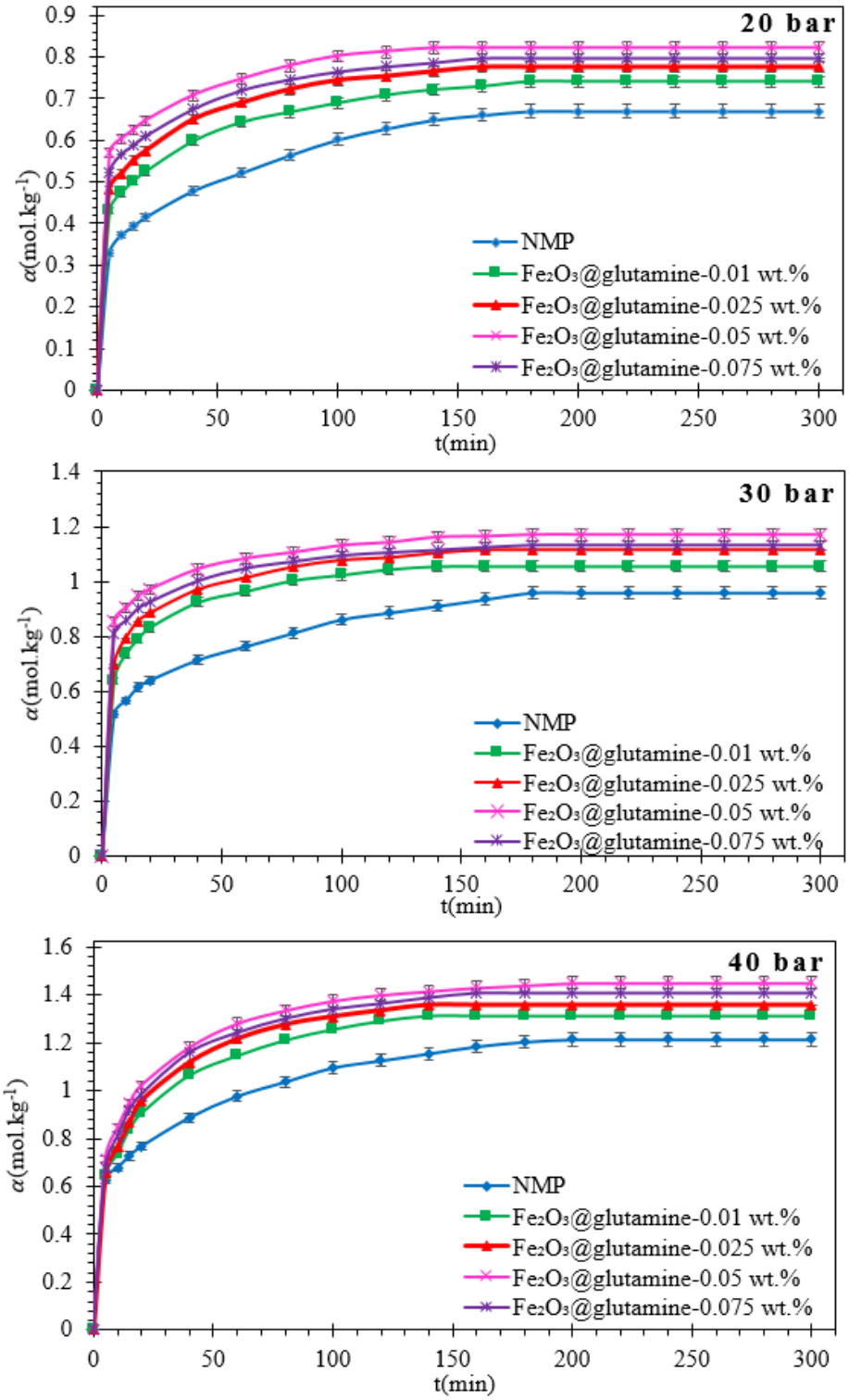

Figure 6

Influence of Fe2O3@glutamine NPs on CO2 absorption of NMP solution at the initial presssure of 20, 30, and 40 bar (T=308 K).

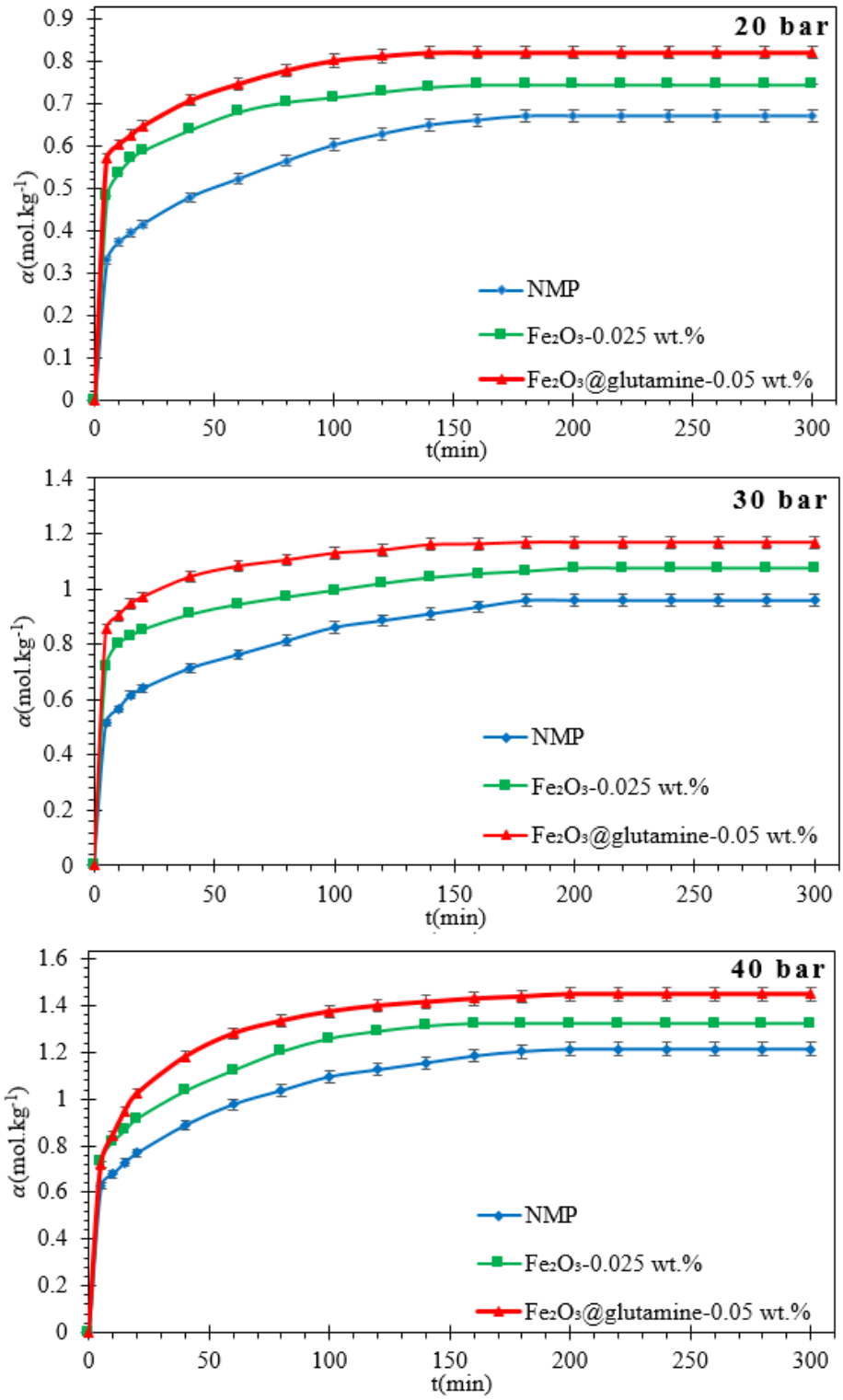

Figure 7

Comparison of optimum concentrations of Fe2O3 and Fe2O3@glutamine nanofluids in CO2 absorption at the initial presssure of 20, 30, and 40 bar (T=308 K).

Supplementary Files

This is a list of supplementary files associated with this preprint. Click to download.

- SupplementaryInformation.docx